Eikonal acceleration technique for studying of the Earth and planetary atmospheres by radio occultation method

A. G. Pavelyev,[1] Y. A. Liou,[2] J. Wickert,[3] A. L. Gavrik,[1] and C. C. Lee[4]

Received 13 September 2009; accepted 12 October 2009; published XX Month 2009.

[1] Lately introduced a phase (eikonal) acceleration technique extends an applicable domain of radio occultation (RO) method and can be applied for identification of the plasma layers in the lower ionosphere. This technique can also convert the eikonal excess or Doppler frequency changes measured in RO experiments into the refractive attenuation variations. From these derived refractive attenuation and amplitude data one can estimate the integral absorption of radio waves. This is important for study of the radio wave propagation effects in the atmospheric telecommunication links and for remote sensing of the atmosphere and ionosphere. The advantages of the eikonal acceleration technique are validated by analyzing the RO data from the Challenging Minisatellite Payload (CHAMP) and Venus missions. **Citation:** Pavelyev, A. G., Y. A. Liou, J. Wickert, A. L. Gavrik, and C. C. Lee (2009), Eikonal acceleration technique for studying of the Earth and planetary atmospheres by radio occultation method, *Geophys. Res. Lett.*, *36*, LXXXXX, doi:10.1029/2009GL040979.

1. Introduction

[2] The radio occultation (RO) method is an effective tool for the investigation of radio waves propagation effects in the trans-atmospheric links and for remote sensing of the Earth's atmosphere and ionosphere at different altitudes with global coverage [e.g., *Hajj and Romans*, 1998, and references therein]. A connection between the eikonal acceleration, Doppler shift, phase, and intensity variations of RO signals has been revealed by theoretical considerations and experimental analysis of the RO radio-holograms [*Liou and Pavelyev*, 2006; *Pavelyev et al.*, 2007, *Liou et al.*, 2007]. The introduced eikonal acceleration technique gives a way to convert the RO phase data into the refractive attenuation and seems to be simpler as compared with the thin phase screen model [*Sokolovskiy*, 2000] and radio-holographic back-propagation method proposed by *Gorbunov et al.* [2002], and *Sokolovskiy et al.* [2002], for determination of the height and location of layered plasma structures in the ionosphere. This technique may be applied also to estimate the integral atmospheric absorption. The absorption measurements are planned for future RO missions [*Kirchengast and Hoeg*, 2004] to determine the water vapor abundance in the stratosphere and troposphere. A differential Canonical Transform/Full Spectrum Inversion (CT/FSI) technique was proposed to retrieve absorption in X/K band, 9–22 GHz [*Gorbunov and Kirchengast*, 2005]. The integral absorption effect in the trans-atmospheric telecommunication link orbital station MIR – geostationary satellites was measured at frequency 930 MHz [*Pavelyev et al.*, 1997]. In this experiment the refractive attenuation has been excluded by use of the phase and Doppler frequency data. *Lohman et al.* [2003] and *Jensen et al.* [2004] detected a possibility to measure absorption in the atmosphere in X/K band by use of a spectral phase matching method (SPMM) and Fourier Integral Operators (FIO). They demonstrated how the second derivative of the phase on time can be used for excluding the refractive attenuation from an amplitude function of the SPMM and FIO spectra. The eikonal acceleration technique can be directly applied to estimation of the integral absorption in the atmosphere from analysis of RO data. In this paper the eikonal acceleration technique is validated by use of CHAMP GPS and Venus RO data, and a method for identification of layered structures in the atmosphere and ionosphere is introduced. A possibility to measure the integral absorption of radio waves at GPS frequency by use of the proposed eikonal acceleration technique is considered.

2. Identification of Layered Structures

[3] The radio waves emitted by a GPS satellite (point G) are propagating to a LEO satellite (point L) along the radio ray trajectory GTL, where T is the ray perigee relevant to a center of spherical symmetry of the atmosphere – point O. Point T is the tangent point where the ray is perpendicular to gradient of refractivity. Point D is projection of point O on the line of sight GL (Figure 1). Point E is projection of point T on the Earth's surface and determines the geographical coordinates of a RO session. *Liou and Pavelyev* [2006], *Pavelyev et al.* [2007], and *Liou et al.* [2007] detected connections between the eikonal excess Φ(p), derivative of the Doppler frequency F_d on time and the power refractive attenuation of radio waves $X_p(t)$:

$$1 - X_p(t) = ma = m\frac{dF_d}{dt} = m\frac{d^2\Phi(p)}{dt^2};\ m = q\left(\frac{dp_s}{dt}\right)^{-2};\quad q = d_1 d_2 R_0^{-1} \qquad (1)$$

where p and p_s are the impact parameters corresponding to the radio ray GTL and the line of sight GDL and d_1 and $d_2$are the distances GD and DL, respectively (Figure 1). Equations (1) are based on an exact 3-D geometrical optics formula for the power refractive attenuation [*Pavelyev and Kucherjavenkov*, 1978; *Eshleman et al.*, 1980; *Kalashnikov et al.*, 1986, *Sokolovskiy*, 2000] and are valid in the case of

[1]Institute of Radio Engineering and Electronics of Russian Academy of Sciences, Fryazino, Russia.
[2]Center for Space and Remote Sensing Research, National Central University, Jhongli, Taiwan.
[3]GeoForschungsZentrum Potsdam, Potsdam, Germany.
[4]General Education Center, Ching Yun University, Jhongli 320, Taiwan.

0094-8276/09/2009GL040979$05.00

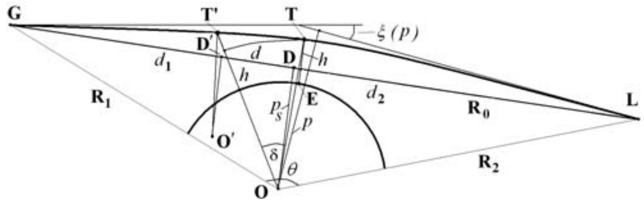

Figure 1. Scheme of trans-atmospheric link satellite-to-satellite.

strong refractive effect and one-ray path propagation under condition $|p - p_s| \ll p_s$ [*Liou et al.*, 2007]. Parameters m and $\frac{dp_s}{dt}$ may be calculated by use of equations:

$$\frac{dp_s}{dt} = [v + (w - v)z]; \ z = d_2 R_0^{-1}; \quad m = R_0 z(1 - z)[v + (w - v)z]^{-2} \qquad (2)$$

Where v and w are the velocity components of the LEO and GPS satellites, respectively, which are perpendicular to the straight line GL in plane GOL. Components w and v are positive when oriented in direction to the point O. Equations (1) and (2) give a possibility to convert the eikonal acceleration a and Doppler frequency F_d to the refractive attenuation X_p. A relationship between the derivative of the refractive angle ξ with respect to time $\frac{d\xi}{dt}$ and X_p follows from 3-D formula for the refractive attenuation:

$$X_p = \left(1 - q\frac{d\xi}{dp}\right)^{-1}, \ \frac{d\xi}{dp} = \frac{d\xi}{X_p dt}\left(\frac{dp_s}{dt}\right)^{-1}, \ \frac{d\xi}{dt} = (X_p - 1)\frac{dp_s}{qdt} \qquad (3)$$

A ratio X_a of the intensities of radio signal propagating through the atmosphere, $I_a(t)$, and free space, I_s:

$$X_a(t) = I_a(t) I_s^{-1} = X_p Y, \qquad (4)$$

is equal to the product of X_p, absorption losses Y, and may include technical instabilities. Comparison of the values of X_a and X_p, calculated from the RO amplitude and phase data (curves 1 and 2) for GPS RO event № 0033 in the altitude intervals 5–30 km and 75–125 km, are shown in Figures 2a and 2b, respectively. The standard dependence of the combined refractive attenuation and atmospheric absorption is indicated in Figure 2b by curve 3. To obtain X_p the eikonal acceleration a has been estimated as the second derivative of the eikonal excess with respect to time t over a fixed time interval Δt, which was equal to 0.42 s. The values X_a and X_p change in similar manners in the stratosphere (Figure 2a) and in the lower ionosphere (Figure 2b). This identifies a common origin of the phase and intensity variations of GPS RO signal as a contribution of layers. As a further identification step a possibility to locate inclined layers may be examined. In the case of an inclined layer the center of spherical symmetry O and tangent point T may be displaced to point O′ and T′, respectively, owing to influence of the horizontal gradients of refractivity. Projection of point O′ on the line of sight GL is located at point D′ (Figure 1). Parameter m corresponding to a layer may be evaluated from the RO amplitude and phase data if the noise and absorption are absent: $m = [1 - X_a(t)]a^{-1}$. For any value m the last equation (2) has two solutions:

$$d_2 = zR_0; \ z = \frac{1 + 2m_1(w - v)v \pm \sqrt{1 - 4m_1 wv}}{2[1 + m_1(w - v)^2]}; \ m_1 = mR_0^{-1} \qquad (5)$$

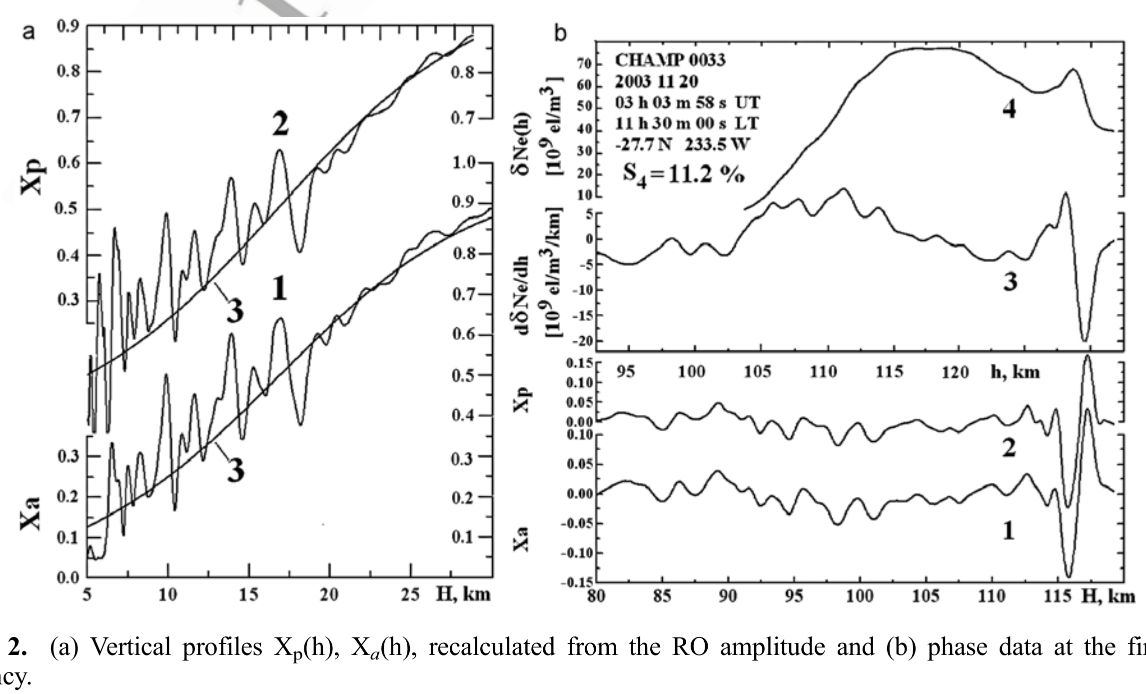

Figure 2. (a) Vertical profiles $X_p(h)$, $X_a(h)$, recalculated from the RO amplitude and (b) phase data at the first GPS frequency.

Table 1. Displacement d in the Neutral Atmosphere

H, km	X_p	X_a	d, km	h, km	$\delta°$	m, s^2/m
9.36	0.32461	0.29659	−5.35	9.36	−0.046	0.43083
9.35	0.32266	0.29152	4.98	9.35	0.044	0.43308
9.33	0.32062	0.28662	14.4	9.35	0.128	0.43515
9.32	0.31833	0.28197	22.3	9.36	0.200	0.43687
9.31	0.31594	0.27761	29.0	9.37	0.258	0.43831
9.30	0.31341	0.27354	34.2	9.39	0.306	0.43945
9.28	0.31069	0.26984	37.7	9.40	0.338	0.44021
9.27	0.30773	0.26645	39.6	9.40	0.354	0.44060
9.26	0.30407	0.26334	38.5	9.38	0.344	0.44035

When $w = v$ the minus sign equation (5) determines a unique point D′ located on the straight GL near the standard position D. This solution may be used for estimation of the layer's location d_2 since in the most RO sessions w and v are of the same order of magnitude:

$$d_2 = 2mv^2[1 + 2mvR_0^{-1}(v - w) + (1 - 4mvwR_0^{-1})^{1/2}]^{-1} \qquad (6)$$

From known value d_2 the layer's inclination δ and corrected height h can be found [*Wickert et al.*, 2004]:

$$\delta = \frac{d}{a+H};\; h = H + \frac{d^2}{2(a+H)};\; d = d_2 - \sqrt{R_2^2 - p_s^2} \qquad (7)$$

where a is the distance OE (Figure 1). Results of determination of the altitude H and parameters X_a, X_p, d, h, δ, m are given in Tables 1 and 2 (columns 1–7, respectively). Data indicated in Tables 1 and 2 correspond to the CHAMP GPS RO event $\mathcal{N}\underline{o}$ 0033. According to Table 1 the displacement d is changing in the −6-km to +40-km interval and corresponding corrections to the altitude H are about 0.1–0.2 km in average in the altitude interval H of 9.14–9.34 km. These results confirm location of atmospheric layers near the ray perigee T (Figure 1). Significant correspondence between the values X_a, X_p is seen also in the interval of 78–120 km (Figure 2b, curves 1 and 2, respectively). Notable variations of the values X_a, X_p in the 78- to 90-km altitude interval of the ray perigee T may be caused by inclined plasma layers in the ionosphere [*Wickert et al.*, 2004; *Pavelyev et al.*, 2007]. According to data in Table 2 the displacement d is changing in the 330-km to 473-km interval and corresponding corrections to the altitude H are about 12 km ± 4 km in average. Results in Table 2 indicate location of sporadic E_s layer at a height of 128 km ± 4 km with displacement d ≈ 420 km from the ray perigee T in the direction TG and inclination about of 2–4°. Application of the Abel transform for retrieving variations in the electron density is justified for locally spherical symmetric medium [*Igarashi et al.*, 2001]. From (3) one can obtain

$$\delta N(p) = -\frac{1}{\pi}\int_p^\infty \frac{d\xi}{dy}\ln\left[\frac{y + \sqrt{y^2 - p^2}}{p}\right]dy$$
$$= -\frac{1}{\pi q}\int_p^\infty (X_a - 1)\frac{dp_s}{dt}\ln\left[\frac{y + \sqrt{y^2 - p^2}}{p}\right]dt, \qquad (8)$$

$$\frac{d\delta N(p)}{dp} = \frac{1}{\pi q p}\int_p^\infty (X_a - 1)\frac{y}{\sqrt{y^2 - p^2}}\frac{dp_s}{dt}dt,$$
$$\frac{dy}{dt} = X_a\frac{dp_s}{dt},\; \frac{d\delta N(p)}{dr} \approx \frac{d\delta N(p)/dp}{[1 - rd\delta N(p)/dp]} \qquad (9)$$

where p is the impact parameter and $\delta N(p)$ is variations in the refractivity. Advantage of relationships (8) and (9) consists in avoiding influence of the upper ionosphere because the refractive attenuation variations are concentrated in a finite altitude interval. The eikonal acceleration may change value X_a in (9) via equations (1) for excluding the possible instabilities in the amplitude. The results of retrieving $\delta Ne(h)$ and $d\delta Ne(h)/dh$ are shown in Figure 2b for RO session 0033. The values X_a and X_p are shown by curves 1 and 2 as function of the altitude of ray perigee H. Curves 1 and 2 agree well. It is another example of the fulfillment (1) for the case of the sporadic E_s layers and significant horizontal gradients. Curves 3 and 4 describe variations $d\delta Ne(h)/dh$ and $\delta Ne(h)$ as functions of the adjusted altitude h. According to curve 3, Figure 2b, the magnitude of $d\delta Ne(h)/dh$ is slowly changing in the interval $\pm 5 \cdot 10^9$ el/m^3/km at altitudes h between 92.5 and 125 km. Sharp variations in the vertical gradient $d\delta Ne(h)/dh$ caused by sporadic Es layer are observed at the altitudes 126–129 km. Integration of the vertical gradient $d\delta Ne(h)/dh$ gives the variations in the electron density $\delta Ne(h)$. The vertical profile of $\delta Ne(h)$ are shown by curve 4 in Figure 2b. The arbitrary integration constant has been chosen according to the IRI model to be equal $40 \cdot 10^9$ el/m^3. The function $\delta Ne(h)$ has two maximums at the altitudes 118 and 128 km. The first maximum corresponds to a smooth behavior of the electron density in the ionospheric E-layer. The second maximum is caused by a sharp sporadic Es-layer located between altitudes 126 and 129 km. This maximum is difficult to observe by the Earth based tools because it has a higher altitude than the first one. This demonstrates the advantage of the eikonal acceleration technique for establishing in some instances the actual location, height, and inclination of sporadic E_s structures from a single RO vertical profile.

[4] The eikonal acceleration technique can be applied to analysis of the RO data obtained during investigation of the planetary ionospheres. An example relevant to the "Venera-15" RO mission conducted in October 1983 is shown in Figures 3a and 3b. The experimental time dependencies of the refractive attenuation X_a and Doppler frequency f(t) obtained during exit of the Venus' satellite "Venera-15" on October 23, 1983, are shown by curves 1 and 2, respectively, in Figure 3a. Comparison of the refractive attenuation

Table 2. Location of an Ionospheric Layer

H, km	$X_p - 1$	$X_a - 1$	d, km	h, km	$\delta°$	m, s^2/m
117.34	0.13934	0.16763	330.1	125.8	2.94	0.60984
117.30	0.14184	0.17263	352.3	127.0	3.14	0.61692
117.26	0.14338	0.17647	373.9	128.1	3.34	0.62383
117.22	0.14384	0.17896	394.9	129.4	3.52	0.63057
117.19	0.14305	0.17996	416.6	130.7	3.72	0.63758
117.15	0.14090	0.17929	439.1	132.2	3.92	0.64485
117.11	0.13757	0.17674	458.1	133.5	4.10	0.65102
117.07	0.13301	0.17214	472.7	134.5	4.22	0.65577

X_a found from the amplitude data and the recalculated Doppler frequency derivative on time df(t)/dt is shown as functions of the perigee height H by curves 1 and 2, respectively, in Figure 3b. The derivative df(t)/dt (curve 2) has been found by a sliding least squares method with averaging in interval 0.28 s. Curve 3 in Figure 3b corresponds to the derivative df(t)/dt found by formula: $df(t)/dt = [f(t_{i+1}) - f(t_{i-1})]/(2\Delta t)$, where Δt was equal to 0.0581 s. The time scales in the Figures 3a and 3b are different; Figure 3b demonstrates the influence of the ionosphere of Venus in detail. The curves 2 and 3 indicate good correspondence between the values X_a and df(t)/dt. This correspondence identifies the layered plasma structures in the ionosphere of Venus.

3. Determination of Integral Absorption

[5] Equations (1) and (2) can be applied to find the integral absorption Y(h) from a ratio $Y(h) = X_a(h)/X_p(h)$. To obtain dependence Y(h) the vertical profiles of $X_a(h)$ and $X_p(h)$ have been approximated by polynomials using a least squares method. In Figure 4 the vertical profiles of $X_p(h)$, $X_a(h)$, and absorption Y(h) are shown by curves 1–5 and 6–10, respectively, for five CHAMP RO measurement sessions conducted in November 20, 2003. For convenience an artificial bias of 0.2 was introduced in consecutive order into the curves 2–5, 6–9, and B. Three sessions –0013, 08 h 42 m of local time (LT), 0096, 11 h 38 m LT, and 0131, 16 h 27 m LT, – correspond to polar and moderate latitude areas in the northern and southern hemispheres, two sessions – 0043, 11 h 16 m LT, and 0033, 11 h 30 m LT, – are relevant to the tropical regions. Therefore, measurements represent conditions of radio wave propagation in typical Earth's regions. Dashed curves A and B correspond to profiles of $X_a(h)$ and Y(h) evaluated from standard atmospheric model. The integral absorption due to atmospheric oxygen Y(h) has been calculated by use of technique described by *Kislyakov and Stankevich* [1967]. At the altitudes between 12 and 30 km the profiles $X_p(h)$ and $X_a(h)$ are nearly coinciding and have good correspondence with the standard profile (curve B). Below 12 km altitude they begin to split (e.g., curves *a* and *p*) at different heights.

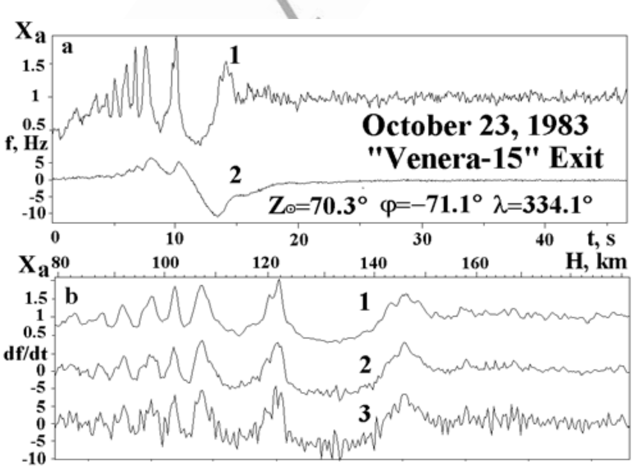

Figure 3. (a) Refraction attenuation $X_a(h)$ and (b) Doppler frequency f(t) [Hz] measured during RO investigation of Venus.

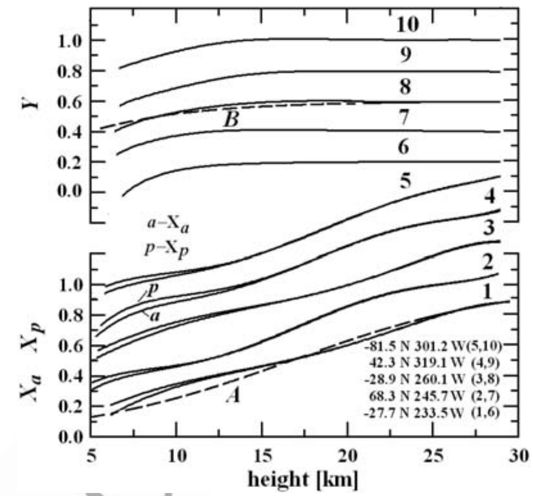

Figure 4. Vertical profiles of $X_p(h)$, $X_a(h)$, and Y(h) (CHAMP RO data). Inserts indicate the geographical coordinates of investigated regions.

The splitting exists practically in all RO events. The difference in the splitting altitude may be connected with amplitude instability. The splitting obviously indicates an influence of the atmospheric integral absorption, which in average is near to the values (curves 6–10 and curve B), described by *Kislyakov and Stankevich* [1967], *Yakovlev et al.* [1995], and *Pavelyev et al.* [1997]. Absorption is changing between 0–30% in the altitude interval 12–5 km (Figure 4, curves 6–10). The value of the amplitude instability error in measured absorption is estimated as ±20% from maximal value. The described results could be of interest for the RO integral absorption measurements at GPS frequencies as a tool for monitoring of the oxygen concentration.

4. Conclusion

[6] Connections between the eikonal acceleration, derivative of the bending angle with respect to time and the refractive attenuation are validated by means of the experimental analysis of data registered during CHAMP and Venus RO missions. These connections convert the eikonal acceleration into the refractive attenuation and allow one to measure the integral absorption of radio waves in the trans-atmospheric communication links. The eikonal acceleration technique may be used to identify and locate layered structures in the Earth's and planetary atmospheres and ionospheres including the case of significant horizontal gradients. In some instances it is possible to establish the location, height, and inclination of E_s structures in the ionosphere from a single RO vertical profile.

[7] **Acknowledgments.** This work was supported by the National Science Council of Taiwan, grant NSC 96-2811-M-008-061, and the NSPO (Taiwan), grant 97-NSPO(B)-SP-FA07-03(F).

References

Eshleman, V. R., D. O. Muhleman, P. D. Nicholson, and P. G. Stesses (1980), Comment on absorbing regions in the atmosphere of Venus as measured by radio occultation, *Icarus*, *44*, 793–798, doi:10.1016/0019-1035(80)90145-1.

Gorbunov, M. E., and G. Kirchengast (2005), Processing X/K band radio occultation data in presence of turbulence, *Radio Sci.*, *40*, RS6001, doi:10.1029/2005RS003263.

Gorbunov, M. E., A. S. Gurvich, and A. V. Shmakov (2002), Back-propagation and radioholographic methods for investigation of sporadic ionospheric *E*-layers from Microlab-1 data, *Int. J. Remote. Sens.*, *23*, 675–685, doi:10.1080/01431160010030091.

Hajj, G. A., and L. J. Romans (1998), Ionospheric electron density profiles obtained with the Global Positioning System: Results from GPS/MET experiment, *Radio Sci.*, *33*, 175–190, doi:10.1029/97RS03183.

Igarashi, K., A. Pavelyev, K. Hocke, D. Pavelyev, and J. Wickert (2001), Observation of wave structures in the upper atmosphere by radio holographic analysis of the RO data, *Adv. Space Res.*, *27*, 1321–1327, doi:10.1016/S0273-1177(01)00144-2.

Jensen, A. S., M. S. Lohmann, A. S. Nielsen, and H.-H. Benzon (2004), Geometrical optics phase matching of radio occultation signals, *Radio Sci.*, *39*, RS3009, doi:10.1029/2003RS002899.

Kalashnikov, I., S. Matugov, A. Pavelyev, and O. Yakovlev (1986), Analysis of the RO method for the Earth's atmosphere study (in Russian), in *Electromagnetic Waves in the Atmosphere and Space*, pp. 208–218, Nauka, Moscow.

Kirchengast, G., and P. Hoeg (2004), The ACE+ Mission: Atmosphere and Climate Explorer based on GNSS-LEO and LEO-LEO radio occultation, in *Occultations for Probing Atmosphere and Climate*, edited by G. Kirchengast, U. Foelsche, and A. K. Steiner, pp. 201–220, Springer, New York.

Kislyakov, A. G., and K. S. Stankevich (1967), Absorption of radio waves in the atmosphere, *Izv. Vyssh. Uchebn. Zaved Radiofiz.*, *10*, 1244–1270.

Liou, Y. A., and A. G. Pavelyev (2006), Simultaneous observations of radio wave phase and intensity variations for locating the plasma layers in the ionosphere, *Geophys. Res. Lett.*, *33*, L23102, doi:10.1029/2006GL027112.

Liou, Y. A., et al. (2007), FORMOSAT-3 GPS radio occultation mission: preliminary results, *IEEE Trans. Geosci. Remote Sens.*, *45*, 3813–3826, doi:10.1109/TGRS.2007.903365.

Lohman, M. S., A. S. Jensen, H. H. Benson, and A. S. Nielsen (2003), Radio occultation retrieval of atmospheric absorption based on FSI, *Rep. 03-22*, Dan. Meteorol. Inst., Copenhagen.

Pavelyev, A. G., and A. I. Kucherjavenkov (1978), Refractive attenuation in the planetary atmospheres, *Radio Eng. Electron. Phys. Engl. Transl.*, *23*, 13–19.

Pavelyev, A. G., et al. (1997), Propagation of radio waves reflected from the Earth's surface at grazing angles between a low-orbit space station and a geostationary satellite, *J. Commun. Technol. Electr.*, *42*, 51–57.

Pavelyev, A. G., et al. (2007), Effects of the ionosphere and solar activity on radio occultation signals: Application to CHAllenging Minisatellite Payload satellite observations, *J. Geophys. Res.*, *112*, A06326, doi:10.1029/2006JA011625.

Sokolovskiy, S. V. (2000), Inversion of radio occultation amplitude data, *Radio Sci.*, *35*, 97–105, doi:10.1029/1999RS002203.

Sokolovskiy, S. V., W. Schreiner, C. Rocken, and D. Hunt (2002), Detection of high-altitude ionospheric irregularities with GPS/MET, *Geophys. Res. Lett.*, *29*(3), 1033, doi:10.1029/2001GL013398.

Wickert, J., A. G. Pavelyev, Y. A. Liou, T. Schmidt, C. Reigber, K. Igarashi, A. A. Pavelyev, and S. Matyugov (2004), Amplitude variations in GPS signals as a possible indicator of ionospheric structures, *Geophys. Res. Lett.*, *31*, L24801, doi:10.1029/2004GL020607.

Yakovlev, O. I., S. S. Matyugov, and I. A. Vilkov (1995), Attenuation and scintillation of radio waves in the Earth's atmosphere in radio occultation experiments on the satellite-to-satellite link, *Radio Sci.*, *30*, 591–600, doi:10.1029/94RS01920.

A. L. Gavrik and A. G. Pavelyev, Institute of Radio Engineering and Electronics, Russian Academy of Sciences, Fryazino 141190, Russia. (pvlv@ms.ire.rssi.ru)

C. C. Lee, General Education Center, Ching Yun University, Jhongli 320, Taiwan. (cclee@cyu.edu.tw)

Y. A. Liou, Center for Space and Remote Sensing Research, National Central University, Chung-Li 320, Taiwan. (yueian@csrsr.ncu.edu.tw)

J. Wickert, GeoForschungsZentrum Potsdam, D-14473 Potsdam Germany. (wickert@gfz-potsdam.de)